



## Accepted Article

**Title:** Design, Synthesis and Bioevaluation of Two Series of 3-((1-Benzyl-1H-1,2,3-triazol-4-yl)methyl)quinazolin-4(3H)-ones and N-(1-benzylpiperidin-4-yl)quinazolin-4-amines

**Authors:** Ta Thu Lan, Duong Tien Anh, Hai Pham-The, Do Thi Mai Dung, Eun Jae Park, Sun Dong Jang, Joo Hee Kwon, Jong Soon Kang, Nguyen Thi Thuan, Sang-Bae Han, and Nguyen-Hai Nam

This manuscript has been accepted after peer review and appears as an Accepted Article online prior to editing, proofing, and formal publication of the final Version of Record (VoR). This work is currently citable by using the Digital Object Identifier (DOI) given below. The VoR will be published online in Early View as soon as possible and may be different to this Accepted Article as a result of editing. Readers should obtain the VoR from the journal website shown below when it is published to ensure accuracy of information. The authors are responsible for the content of this Accepted Article.

**To be cited as:** *Chem. Biodiversity* 10.1002/cbdv.202000290

**Link to VoR:** <https://doi.org/10.1002/cbdv.202000290>

# Design, Synthesis and Bioevaluation of Two Series of 3-((1-Benzyl-1H-1,2,3-triazol-4-yl)methyl)quinazolin-4(3H)-ones and N-(1-benzylpiperidin-4-yl)quinazolin-4-amines

Ta Thu Lan,<sup>a</sup> Duong Tien Anh,<sup>a</sup> Hai Pham-The,<sup>a</sup> Do Thi Mai Dung,<sup>a</sup> Eun Jae Park,<sup>b</sup> Sun Dong Jang,<sup>b</sup> Joo Hee Kwon,<sup>c</sup> Jong Soon Kang,<sup>c</sup> Nguyen Thi Thuan,<sup>\*,a</sup> Sang-Bae Han,<sup>\*,b</sup> Nguyen-Hai Nam<sup>\*,a</sup>

<sup>a</sup>Hanoi University of Pharmacy, 13-15 Le Thanh Tong, Hanoi, 10000, Vietnam

<sup>c</sup>College of Pharmacy, Chungbuk National University, 194-31, Osongsangmyung-1, Heungdeok, Cheongju, Chungbuk, 28160, Republic of Korea

<sup>d</sup>Bio-Evaluation Center, Korea Research Institute of Bioscience and Biotechnology, Cheongju, Chungbuk, 28116, Republic of Korea

\*Corresponding authors: Tel.: +84-4-39330531; Fax: +84-4-39332332; Emails: namnh@hup.edu.vn (N.H. Nam).

Two series of 3-((1-benzyl-1H-1,2,3-triazol-4-yl)methyl)quinazolin-4(3H)-ones (**4a-j**) and N-(1-benzylpiperidin-4-yl)quinazolin-4-amines (**6a-j**) were designed initially as potential acetylcholine esterase inhibitors. Biological evaluation demonstrated that series **6a-j** significantly inhibited AChE activity. Especially compounds **6c** and **6e** were found to be the most potent with relative AChE inhibition percentages of 87% in comparison to donepezil. The docking studies with AChE showed similar interactions between Donepezil and these four derivatives. Compounds **6a-j** also exhibited significant DPPH scavenging effects. Two compound series also exerted moderate to good cytotoxicity againsts three human cancer cell lines, including SW620 (human colon cancer), PC-3 (prostate cancer), and NCI-H23 (lung cancer), with compound **4a** being the most cytotoxic agent. Compound **4a** significantly induced early apoptosis and arrested the SW620 cells at G2/M phase. From this study, compounds **6c** and **6e** could serve as new leads for further design and AChE inhibitors, while compound **4a** could serve as a new lead for the design and development of more potent anticancer agents.

**Keywords:** Acetylcholine esterase inhibitors • quinazolin-4(3H)-one, quinazolin-4-amine • cytotoxicity • docking simulation

## Introduction

Alzheimer's disease (AD) is one the most common form of dementia.<sup>[1]</sup> It is an age-related neurodegenerative disorder and accounts for approximately 80% of dementia patients worldwide. Clinically, the disease is characterized by a progressive loss of memory and impairment of cognitive functions.<sup>[1, 2]</sup> Currently, the disease is estimated to affect nearly 30 million individuals of people over the age of 65.

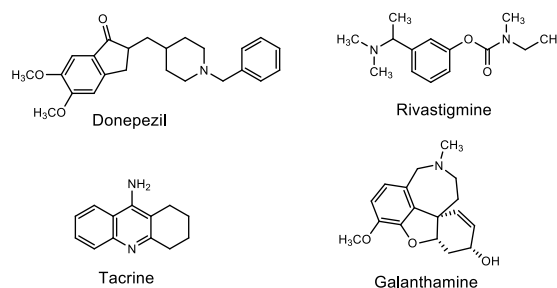


Figure 1. Structures of some AChE inhibitors.

Despite enormous efforts of scientists devoted in studying the AD's pathology, the primary causes of the disease has not yet been completely understood. It is, therefore, AD remains one of the incurable neurological disorders to date and the treatment of the disease remains symptomatic treatment.<sup>[1]</sup> Pathologically, a number of researches have indicated that several factors, such as abnormal posttranslational modifications of tau protein resulting in neurofibrillary tangles, deposition of amyloid  $\beta$ -protein ( $A\beta$ ) plaques, and a

## Chem. Biodiversity

decrease in the level of the neurotransmitter acetylcholine, are closely associated with AD's initiation and progression.<sup>[3,4]</sup> Therapeutically, acetylcholine esterase inhibitors are still the only class of drugs approved for treatment of AD hitherto. Donepezil, tacrine, galanthamine and rivastigmine (Figure 1) are some acetylcholine esterase inhibitors which have been shown to induce significant improvements in memory and cognitive functions.<sup>[5]</sup>

Acetylcholine esterase (AChE; EC 3.1.1.7) belongs to the serine hydrolase enzyme class. These enzymes catalyze the hydrolysis of acetylcholine, a neurotransmitter, to liberate choline and acetic acid, leading to the termination of cholinergic neurotransmission.<sup>[6]</sup> Inhibition of acetylcholine esterase, therefore, prevents the breakdown of acetylcholine and boosts cholinergic neurotransmission, resulting in clinical benefits. Due to its therapeutic importance, medicinal chemists worldwide have devoted great efforts in developing novel AChE inhibitors. As a result, numerous AChE inhibitors have been described in the past decades, both naturally and synthetic.<sup>[7]</sup> In our research program to develop novel AChE inhibitors we have used fragment-hopping and structural similarity approach coupled with docking probe to design a series of donepezil analogues (Figure 2). This paper describes the synthesis and evaluation of AChE inhibitory activity of this compounds series. The free radical scavenging effects of these compounds were also evaluated. In addition, since the compounds possess quinazoline ring which is present in many anticancer agents, the cytotoxicity of the compounds against some human cancer cell lines was also reported.

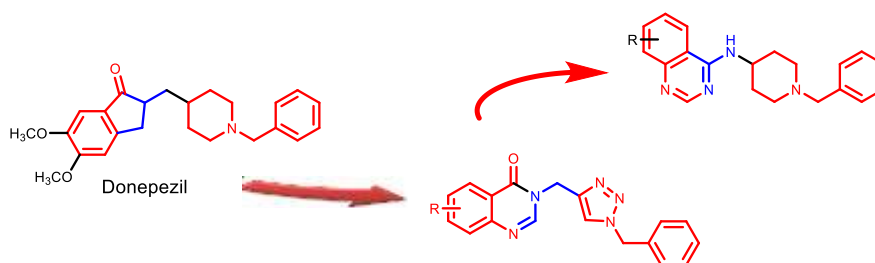


Figure 2. Design of novel quinazoline derivatives as potential AChE inhibitors.

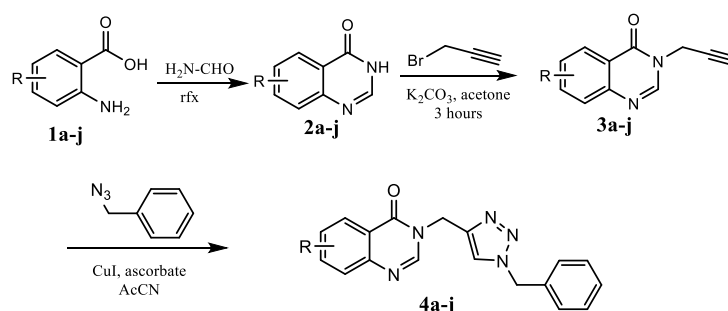
## Results and Discussion

### Chemistry

The target 3-((1-benzyl-1*H*-1,2,3-triazol-4-yl)methyl)quinazolin-4(3*H*)-ones (**4a-j**) were synthesized via a three-step pathway, as illustrated in Scheme 1. Condensation of the anthranilic acids (**1a-j**) with formamide under high temperature gave quinazolin-4(3*H*)-ones (**2a-j**) in good yields (80-95%). Nucleophilic substitution reaction of compounds **2a-j** with propargyl bromide under basic conditions ( $K_2CO_3$ ) in acetone with a catalytic amount of KI gave exclusively the 3-propargylquinazolin-4(3*H*)-ones (**3**) in quantitative yields (85-94%). Finally, a Click reaction of the intermediates **3a-j** with benzyl azide was cleanly proceeded using CuI and ascorbate in acetonitrile to give 3-((1-benzyl-1*H*-1,2,3-triazol-4-yl)methyl)quinazolin-4(3*H*)-ones (**4a-j**) in moderate to good yields (65-87%).

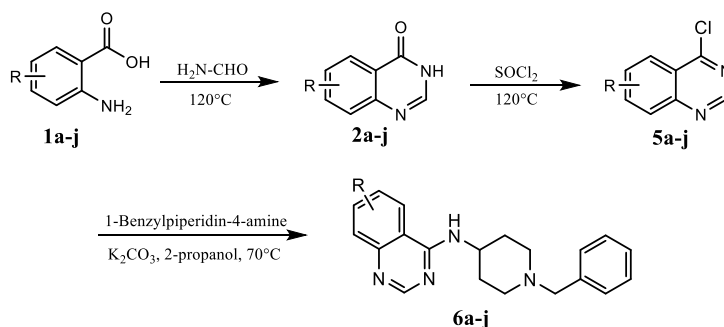
Compounds **6a-j** were synthesized via a three-step pathway, also from anthranilic acids (**1a-j**), as illustrated in Scheme 2. The quinazolin-4(3*H*)-ones (**2a-j**) were first chlorinated at position 4 to give 4-chlorinated intermediates **5a-j** in good yields (75-84%). The intermediates **5a-j** were then reacted with 1-benzylpiperidin-4-amine in 2-propanol under basic conditions to afford target compounds **6a-j** in moderate yields (60-63%).

The structures of the synthesized compounds **4a-j** and **6a-j** were determined straightforwardly based on analysis of spectroscopic data, including IR, MS,  $^1H$  and  $^{13}C$  NMR.



## Chem. Biodiversity

Scheme 1. Synthesis of 4-oxoquinazoline derivatives 4a-j



Scheme 2. Synthesis of quinazoline derivatives 6a-j.

**Bioactivity**

The AChE inhibitory effects of the synthesized compounds **4a-j** and **6a-j** were screened at 50  $\mu\text{M}$ . The AChE inhibitor screening kit (colorimetric, BioVision (catalog #K197-100)) was used for the evaluation. The absorbance was kinetically measured at 412 nm for 40 min. The results expressed as the enzyme relative inhibition percentages in comparison to donepezil, a positive control, at the final point are shown in Figure 3. All compounds in series **4a-j** showed no or only negligible effects on the AChE activity. Interestingly, compounds in series **6a-j** exhibited very noted inhibitory activity with relative inhibition percentages up to 87% in comparison to donepezil. Compounds **6c** (with 7- $\text{CH}_3$  substituent) and compound **6e** (with 6,7- $(\text{OCH}_3)_2$  substituent) were two most potent AChE inhibitors in series **6a-j** (relative inhibition percentages up to 87%). Compound **6b** (with 6- $\text{CH}_3$  substituent) also displayed strong AChE inhibition (relative inhibition percentage, 80%). The two fluorinated compounds **6f** and **6g** were the next most potent AChE inhibitors in series **6a-j** (relative inhibition percentages were 67 and 77%, respectively). Thus, it is clear that series **6a-j**, especially compounds **6b**, **6c**, **6e**, and **6g**, were promising AChE inhibitors. It could be easily noted that compounds **6a-j** possess structurally features similar to donepezil, which are likely attributable for their potent AChE inhibitory effects, while compounds in series **4a-j** did not show any significant activity.

Since antioxidant activity would be an added value for AChE inhibitors to treat Alzheimer, we decided to evaluate compounds **6a-j** for their DPPH scavenging activity using a method previously described by Ellman et al.<sup>[8]</sup> The results illustrated in Figure 4 demonstrate that compounds **6a-j** also exhibited moderate DPPH scavenging activity. Among the compounds in the series, compound **6e** was the most potent DPPH scavenger with an inhibition percentage of 64.4%. It could be observed that compounds bearing electron donating groups on the quinazoline ring (**6b-e**) displayed stronger DPPH scavenging activity in comparison to compounds with electron withdrawing substituents (**6f-j**). Thus, electron density would be a factor important for the DPPH scavenging activity of the compounds in series **6a-j**.

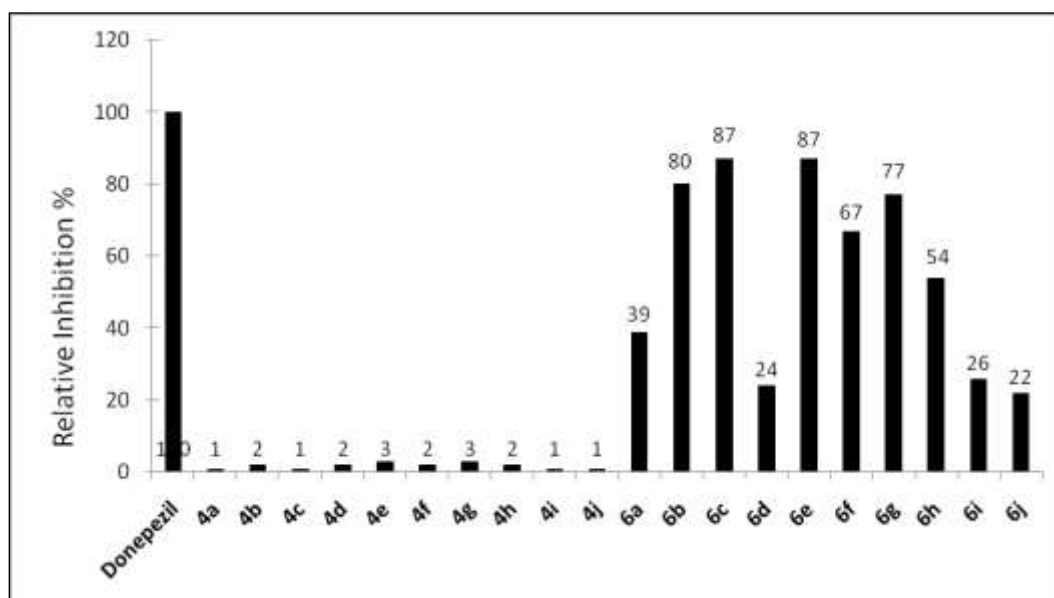


Figure 3. Relative inhibition of AChE by the compounds synthesized in comparison to donepezil. The enzyme was treated with samples at 50  $\mu\text{M}$  and donepezil at 20  $\mu\text{M}$ .

## Chem. Biodiversity

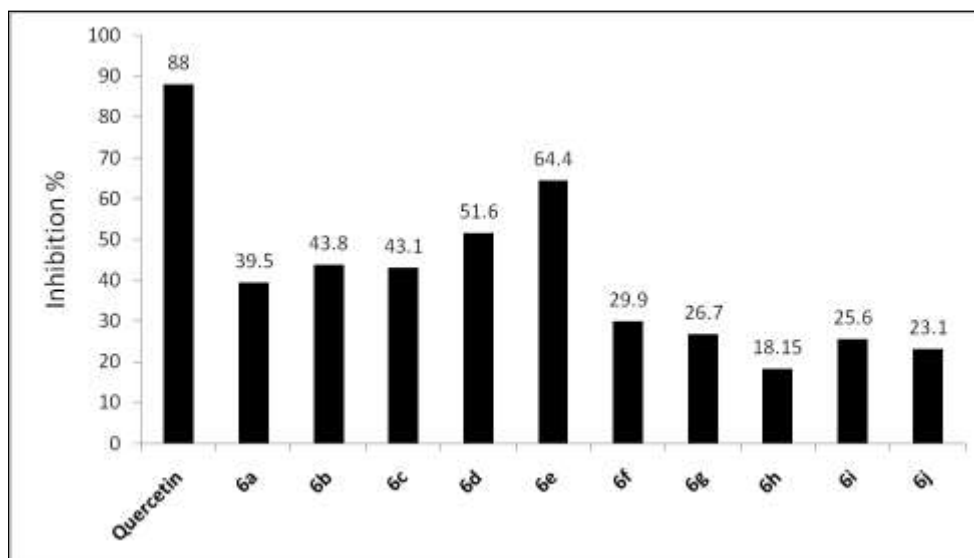
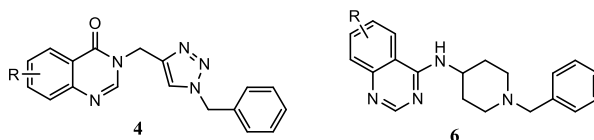


Figure 4. DPPH scavenging activity of compounds 6a-j. The compounds were assayed at 50 µg/mL. Quercetin (50 µg/mL) was used as a positive control.

Structurally, compounds 4a-j and 6a-j possess a 4-oxoquinazoline or quinazoline scaffolds, which are known to be present in various anticancer agents.<sup>[8]</sup> Therefore, in addition to AChE inhibitory and DPPH scavenging activities, we also screened these compounds for their cytotoxicity against three human cancer cell lines, including SW620 (colon cancer), PC-3 (prostate cancer), and NCI-H23 (lung cancer). SRB method was used. The results are summarized in Table 1. It was found that compounds in series 4a-j were generally more cytotoxic than compounds in series 6a-j. In series 4a-j, only two compounds 4a and 4e showed IC<sub>50</sub> values higher than 10 µM in three human cancer cell lines tested. Eight other compounds (4a-c, 4f-j) displayed lower IC<sub>50</sub> values (1.56-8.64 µM). These compounds were found to be stronger in term of cytotoxicity in comparison to 5-FU, a current widely used anticancer agent. Within two series 4a-j and 6a-j, three compounds 4a, 4h, and 4i, especially compound 4a, emerged as the most cytotoxic compound and this compound could serve as a new lead to further design more potent anticancer agents.

Table 1. Cytotoxicity of the synthesized compounds in some human cancer cell lines



Compound	R	MW	LogP <sup>[a]</sup>	Cytotoxicity (IC <sub>50</sub> <sup>[b]</sup> µM)/Cell lines <sup>[c]</sup>		
				SW620	PC3	NCI-H23
4a	H	317.35	2.21	2.21±0.011	1.56±0.103	2.01±0.213
4b	6-CH <sub>3</sub>	331.38	2.76	4.80±0.044	3.22±0.240	2.69±0.268
4c	7-CH <sub>3</sub>	331.38	2.76	5.67±0.094	5.65±0.216	6.05±0.408
4d	7-OCH <sub>3</sub>	347.38	2.29	11.12±0.481	10.23±0.871	12.34±0.921
4e	6,7-(OCH <sub>3</sub> ) <sub>2</sub>	337.40	1.85	10.42±0.321	11.32±0.723	11.33±0.862
4f	6-F	335.34	2.41	5.55±0.094	3.34±0.148	5.05±0.466
4g	7-F	335.34	2.41	8.64±0.173	7.03±0.428	5.67±0.152
4h	6-Cl	351.79	2.85	3.07±0.203	2.72±0.272	3.61±0.054
4i	6-Br	396.25	3.10	3.45±0.098	3.16±0.092	2.14±0.001
4j	6-I	443.25	3.38	5.57±0.282	4.10±0.219	4.86±0.380
6a	H	318.42	3.96	14.34±1.014	13.21±1.341	12.23±1.341
6b	6-CH <sub>3</sub>	332.45	4.50	18.34±1.936	13.76±1.213	14.23±1.081
6c	7-CH <sub>3</sub>	332.45	4.50	15.21±1.012	9.23±0.903	11.23±0.902
6d	7-OCH <sub>3</sub>	348.45	4.04	21.35±2.011	18.56±1.761	20.47±1.121
6e	6,7-(OCH <sub>3</sub> ) <sub>2</sub>	378.48	3.60	>30	>30	>30

## Chem. Biodiversity

6f	6-F	336.41	4.16	13.23±0.911	18.31±1.012	18.27±0.971
6g	7-F	336.41	4.16	15.32±0.912	17.21±1.901	15.31±1.071
6h	6-Cl	352.87	4.60	16.21±1.021	20.54±1.705	24.23±2.010
6i	6-Br	396.32	4.85	17.56±1.311	22.54±0.901	19.49±1.971
6j	6-I	444.32	5.12	20.76±1.901	15.21±0.121	27.32±2.012
5-FU <sup>[d]</sup>		130.08	-0.81	8.84±1.92	13.61±0.46	13.45±3.92
ADR <sup>[e]</sup>		543.5	1.27	1.12±0.14	1.16±0.28	1.29±0.12
SAHA <sup>[f]</sup>		264.32	1.44	1.12±0.10	1.82±0.09	1.44±0.17

<sup>[a]</sup>Calculated by KowWin v.167 program; <sup>[b]</sup>The concentration ( $\mu\text{M}$ ) of compounds that produces a 50% reduction in enzyme activity or cell growth, data represent means  $\pm$  standard errors of the mean (SEM) of triplicate experiments ( $n = 3$ ); <sup>[c]</sup>Cell lines: SW620, colon cancer; PC3, prostate cancer; NCI-H23, lung cancer; <sup>[d]</sup>5-FU: 5-Fluorouracil, a positive control. <sup>[e]</sup>5-ADR: Adriamycin, a positive control. <sup>[f]</sup>SAHA: vorinostat, an anticancer agent acting by inhibition of histone deacetylase, used as a positive control.

With the results from the SRB assays, we selected compound **4a** for flow cytometry analysis to see whether the compound affect the cell cycle. SW620 cells were used for this experiment. The cells were initially pre-incubated for 24 h. Then, the cells were treated with compound **4a** (10  $\mu\text{M}$ ) or SAHA (1  $\mu\text{M}$ ) for 24 h. After that, the cells were harvested and the DNA contents were analyzed. It was found that compound **4a** killed a substantial population of cells at Go/G1 phase (27.40%). Among the viable cells, compounds caused a large population of cells at G2/M phase (29.52%, vs. 5.31% of the VH) (Figure 5). Thus, it was clear that compound **4a** arrested cell cycle of SW620 cells at G2/M phase. This was in contrast to the effects of SAHA, which caused SW620 cells arrest at Go/G1 phase (Figure 5).

Next, the Annexin V-FITC/PI dual staining assay was used to determine whether compound **4a** induced apoptosis in SW620 cells. SW620 human colon cancer cells were plated in 6-well culture plates and allowed to grow for 24 h. The cells were treated with compound **4a** at 30  $\mu\text{M}$  for 24 h, then harvested. The harvested cells were washed twice with ice-cold PBS and incubated in the dark at room temperature in 100  $\mu\text{l}$  of 1 $\times$  binding buffer containing 1  $\mu\text{l}$  Annexin V-FITC and 12.5  $\mu\text{l}$  PI. The results clearly demonstrated that compound **4a** significantly induced early apoptosis (stained red with Annexin V) (Figure 6).

In good consistence with the effects of the compound **4a** on the cell cycle and apoptosis, the morphology of SW620 colon cancer cells was substantially changed similar to that caused by SAHA, a positive control (Figure 7).

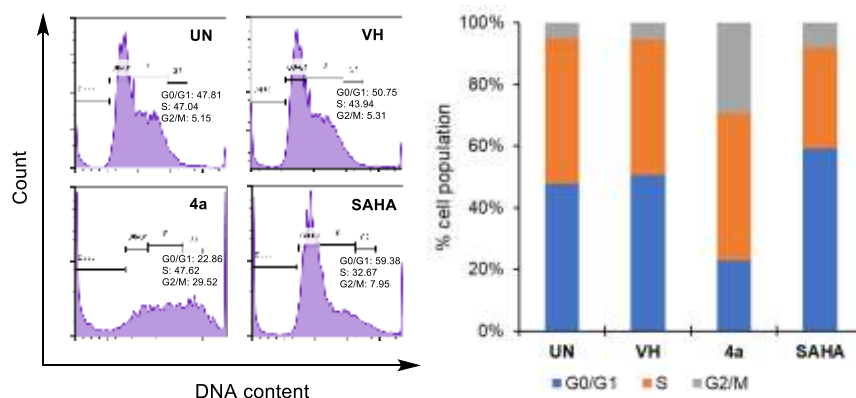
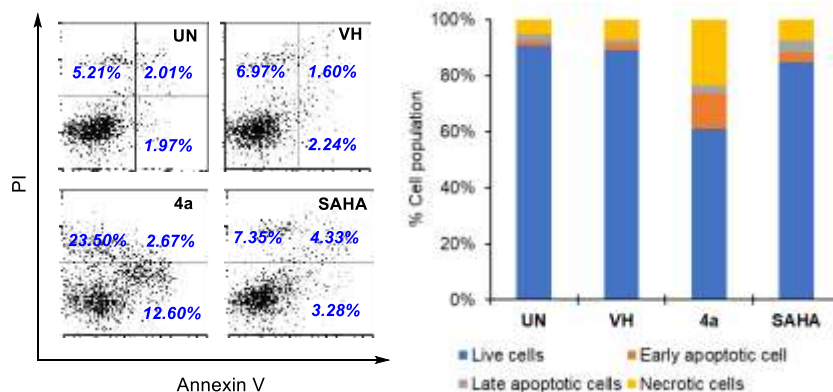


**Figure 5.** Cell cycle analysis of representative compounds **4a**. SW620 cells (human colon cancer) ( $2 \times 10^5$  cells) were treated with compound (30  $\mu\text{M}$ ) or SAHA (a positive control) (1  $\mu\text{M}$ ) for 24 h. The harvested cells were stained with propidium iodide (PI) in the presence of RNase and then were analyzed for DNA content. UN: untreated, VH: vehicle (DMSO, 0.05%). Data was represented as histograms (left) and bar graphs (right).



## Chem. Biodiversity

**Figure 6.** Apoptosis (Annexin V/PI) analysis of representative compounds **4a**. SW620 cells (human colon cancer) ( $2 \times 10^5$  cells) were treated with compound ( $30 \mu\text{M}$ ) or SAHA (a positive control) ( $1 \mu\text{M}$ ) for 24 h. The harvested cells were stained with propidium iodide (PI) in the presence of RNase and then were analyzed for DNA content. UN: untreated, VH: vehicle (DMSO, 0.05%). Area 1 = PI positive population, Area 2: Annexin V-positive population. Data was represented as histograms (left) and bar graphs (right).

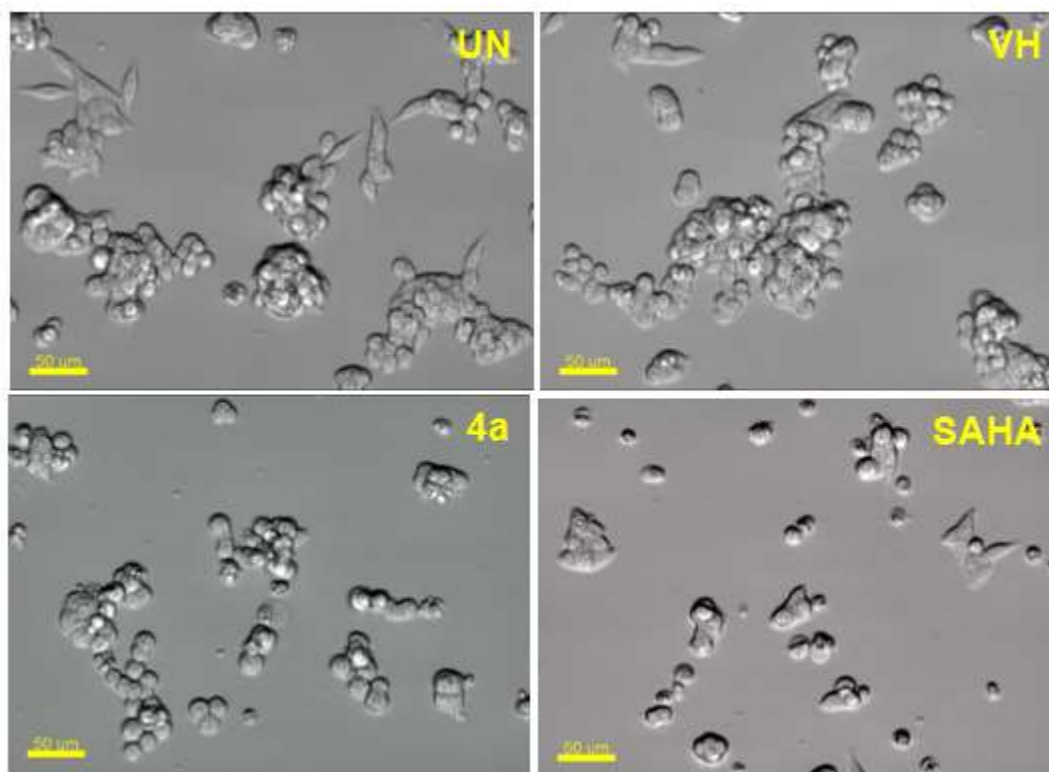


**Figure 7.** Morphology changes of cells treated with representative compound **4a**. SW620 (human colon cancer) cells ( $2 \times 10^5$  cells/well in 6-well plate, pre-incubated for 2 h) were treated with compounds ( $30 \mu\text{M}$ ) or SAHA (a positive control) ( $1 \mu\text{M}$ ) for 24 h. Then, the cells were photographed using an Imaging Device: Biostation with 20X lens. Scale bar: 50  $\mu\text{m}$ .

### Molecular docking studies

In this study several 3-((1-benzyl-1*H*-1,2,3-triazol-4-yl)methyl)quinazolin-4(3*H*)-ones and *N*-(1-benzylpiperidin-4-yl)quinazolin-4-amines were synthesized and evaluated inhibitory activity against AChE enzyme. Some of them (**6b**, **6c**, **6e** and **6g**) show good relative inhibition (77-87%) against AChE in comparison with donepezil. To better understand the difference between tested compounds and donepezil, as well as to investigate the structure-activity relationships of AChE inhibitors, semi-flexible docking simulations were performed using ICM Pro 3.8 software.<sup>[9]</sup> A crystal complex of AChE-Donepezil reported by Cheung et al. was used for this study.<sup>[10]</sup> There are controversial literatures related to the role of water molecule in forming tight hydrogen bonds between the heterocyclic amine like piperidine ring of Donepezil toward key residues such as Tyr341 and Tyr337 of AChE. We then adopted the docking protocol reported by Roberts and Mancera,<sup>[11]</sup> with a slight modification by removing water molecules in the binding site for docking assays.<sup>[12]</sup>

In order to demonstrate the validity of docking protocol, donepezil was firstly redocked into the active site of AChE. As the results, the binding orientations of the redocked and co-crystal structures were highly overlapped (RMSD = 0.397Å). As can be seen in Figure 8A, the key hydrogen bonding interaction between Donepezil with Phe295 of AChE was conserved. This interaction is important to accommodate indanone ring at the peripheral anionic site (PAS) of AChE.<sup>[13]</sup> In addition, the phenyl moiety of donepezil could interact with the choline-binding site and forms multiple  $\pi$ - $\pi$  stacking interactions with Trp86 aromatic side chain. The affinity score calculated for donepezil was -27.67 kCal/mol. The results obtained are suitable and the applied protocol could be utilized for further docking studies.

## Chem. Biodiversity

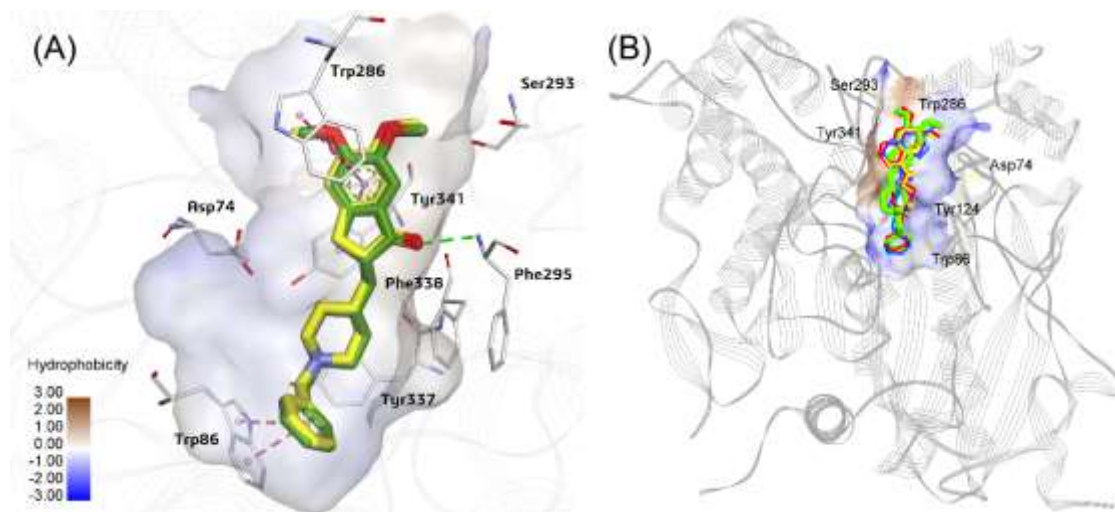


**Figure 8.** Superposition between: (A) redocked donepezil (yellow carbon), and (B) synthesized compounds (**6b**, **6c**, **6e**, **6g** represent as colored molecules) and co-crystal Donepezil (green carbon).

The next step involved into docking four derivatives (**6b**, **6c**, **6e** and **6g**) into the binding site of AChE following the protocols described previously. Being illustrated in the Figure 8B, all four compounds showed similar interactions as donepezil. Compound **6e** exhibited the highest affinity with AChE compared to the other derivatives. The docking scores determined for four **6b**, **6c**, **6e** and **6g** were -26.50, -26.91, -27.38, and -25.73 kCal/mol, respectively, slightly lower than that of donepezil. The docking scores agreed well with the ranking order of in vitro values. For all the compounds, the quinazoline moiety formed multiple stacking interactions with Trp286 and Tyr341. These interactions were similar to indanone ring of donepezil as shown in Figure 8A and played important role for stabilizing the ligand on the entrance of the PAS cavity. Figure 9 showed an interaction comparison of two most active compounds (**6c** and **6e**). Compound **6e** formed two hydrogen bonds with Tyr124 and Phe295, and the remaining interactions were almost identical. Meanwhile for **6c**, the distance between the quinazoline ring and NH backbone of Phe295 was pushed as far as 4.26 Å and it could not form hydrogen bond with that residue. The lack of that hydrogen bond may affect the affinity of compound **6c** in comparison with **6e**. In addition, the 6,7-dimethoxy substituents clearly improved the interactions of quinazoline rings with the periphery site of AChE enzyme.

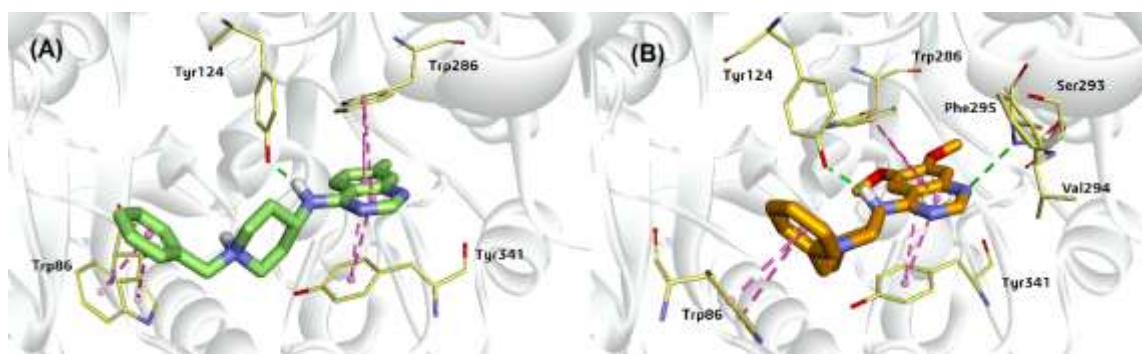


**Figure 9.** Binding pose of compound **6c** (A) and **6e** (B) in the active binding site of AChE

## Conclusions

In this study, we have designed and synthesized two novel series of 3-((1-benzyl-1*H*-1,2,3-triazol-4-yl)methyl)quinazolin-4(3*H*)-ones (**4a-j**) and *N*-(1-benzylpiperidin-4-yl)quinazolin-4-amines (**6a-j**). Series **6a-j** were found to significantly inhibit AChE activity, especially compounds **6c** and **6e** were the most potent with relative AChE inhibition percentages of 87% in comparison to Donepezil. We performed docking studies for these four derivatives and the results showed similar interaction to donepezil. Among them, compound **6e** exhibited the highest affinity with a score of -27.38 kCal/mol. Compounds **6a-j** also exhibited significant DPPH scavenging effects, which would be an added value for these compounds as potential agents to treat AD. Two compound series also exerted moderate to good cytotoxicity against three human cancer cell lines, including SW620 (human colon cancer), PC-3 (prostate cancer), and NCI-H23 (lung cancer), with compound **4a** being the most cytotoxic agent. Compound **4a** significantly induced early apoptosis and arrested the SW620 cells at G2/M

## Chem. Biodiversity

phase. Thus, from this study, compounds **6c** and **6e** could serve as new leads for further design and AChE inhibitors, while compound **4a** could serve as a new lead for the design and development of more potent anticancer agents.

## Experimental Section

### Chemistry

Thin layer chromatography which was performed using Whatman® 250 µm Silica Gel GF Uniplates and visualized under UV light at 254 nm, was used to check the progress of reactions and preliminary evaluation of compounds' homogeneity. Melting points were measured using a Gallenkamp Melting Point Apparatus (LabMerchant, London, United Kingdom) and are uncorrected. Purification of compounds was carried out using crystallization methods and/or open silica gel column flash chromatography employing Merck silica gel 60 (240 to 400 mesh) as stationary phase. Nuclear magnetic resonance spectra (<sup>1</sup>H NMR) were recorded on a Bruker 500 MHz spectrometer with DMSO-*d*<sub>6</sub> as solvent unless otherwise indicated. Tetramethylsilane was used as an internal standard. Chemical shifts are reported in parts per million (ppm), downfield from tetramethylsilane. Mass spectra with different ionization modes including electron ionization (EI), Electrospray ionization (ESI), were recorded using PE Biosystems API2000 (Perkin Elmer, Palo Alto, CA, USA) and Mariner® (Azco Biotech, Inc. Oceanside, CA, USA) mass spectrometers, respectively. The elemental (C, H, N) analyses were performed on a Perkin Elmer model 2400 elemental analyzer. All reagents and solvents were purchased from Aldrich or Fluka Chemical Corp. (Milwaukee, WI, USA) or Merck unless noted otherwise. Solvents were used directly as purchased unless otherwise indicated.

The synthesis of novel compounds **4a-j** and **6a-j** was carried out as illustrated in Schemes 1 and 2. Details are described below.

#### General procedures for the synthesis of compounds **4a-j**

A solution of a respective 2-aminobenzoic acid (**1a-j**) (2 mmol) in excess amount of formamide (4 mL) was stirred at 120 °C for 6 hours. After completion of the reaction, the resulting mixture was cooled and poured into ice-cold water (10 mL). A solution of NaHCO<sub>3</sub> 5% was gradually added to adjust pH to 7, which led to the formation of white solids. The solids were filtered and dried to give the corresponding quinazolinone derivative **2**, which was used for the next step without further purification.

To a respective solution of compounds **2a-j** (1 mmol) in DMF (3 mL) were added K<sub>2</sub>CO<sub>3</sub> (165.5 mg, 1.2 mmol). The mixtures were stirred at 80°C for 1 hour, then then a catalytic amount of KI (8.3 mg, 0.05 mmol) was added. After stirring for further 15 minutes, 0.15 ml of a solution of propargyl bromide 80% in toluene was dropped slowly into the mixtures. The reaction mixtures were again stirred at 60°C for 3 hours. The reaction was checked by TLC. After the reaction completed, the resulting mixtures were cooled, poured into ice-cold water and acidified to pH~4. The white solids formed were filtered and dried to give the propargylated compounds **3**, which were used for the next step without further purification.

A respective solution of compounds **3a-j** and (azidomethyl)benzene (0.5 mmol) in acetonitrile (10 mL) were stirred at room temperature for 10 minutes, then CuI (10 mg, 0.05 mmol) was added. The mixture was stirred at 60°C until the reaction completed (12-24 hours). The corresponding resulting mixtures were evaporated under reduced pressure to give the residues, which were re-dissolved in 50 ml of DCM. The mixtures were filtered and the DCM layers were evaporated under reduced pressure to give the targeting compounds **4a-j**.

#### **3-((1-Benzyl-1H-1,2,3-triazol-4-yl)methyl)quinazolin-4(3H)-one (4a)**

White solid; Yield: 68%. mp: 169-170 °C. *R*<sub>f</sub> = 0.67 (DCM : MeOH = 14 : 1). IR (KBr, cm<sup>-1</sup>): 3138, 3061 (CH, arene); 2941 (CH, CH<sub>2</sub>); 1676 (C=O); 1609, 1474 (C=C). <sup>1</sup>H-NMR (500 MHz, DMSO-*d*<sub>6</sub>, ppm): δ 8.61 (1H, s, H-2); 8.24 (1H, s, H-6'); 8.15 (1H, d, *J* = 8.00 Hz, H-5); 7.84 (1H, t, *J* = 7.50 Hz, H-7); 7.77 (1H, d, *J* = 7.50 Hz, H-8); 7.56 (1H, t, *J* = 7.50 Hz, H-6); 7.40-7.31 (5H, m, H-3", H-4", H-5", H-6", H-7"); 5.57 (2H, s, H-1"a, H-1"b); 5.30 (2H, s, H-1'a, H-1'b). <sup>13</sup>C NMR (125 MHz, DMSO-*d*<sub>6</sub>, ppm): δ 160.30, 148.67, 148.15, 136.21, 134.96, 129.23, 129.19, 128.91, 128.68, 128.63, 128.53, 127.74, 126.56, 124.66, 122.03, 54.07, 53.44, 41.62, 31.16. ESI-MS *m/z*: 318.00 [M+H]<sup>+</sup>.

#### **3-((1-Benzyl-1H-1,2,3-triazol-4-yl)methyl)-6-methylquinazolin-4(3H)-one (4b)**

White solid; Yield: 65%. mp: 175-176 °C. *R*<sub>f</sub> = 0.68 (DCM : MeOH = 14 : 1). IR (KBr, cm<sup>-1</sup>): 3113, 3067 (CH, arene); 2986 (CH, CH<sub>2</sub>); 1657 (C=O); 1603, 1454 (C=C). <sup>1</sup>H-NMR (500 MHz, DMSO-*d*<sub>6</sub>, ppm): δ 8.40 (1H, s, H-2); 8.06 (1H, s, H-6'); 7.85 (1H, s, H-5); 7.57 (1H, dd, *J* = 8.25 Hz, *J*' = 1.75 Hz, H-7); 7.51 (1H, d, *J* = 8.50 Hz, H-8); 7.29-7.21 (5H, m, H-3", H-4", H-5", H-6", H-7"); 5.47 (2H, s, H-1"a, H-1"b); 5.16 (2H, s, H-1'a, H-1'b); 2.35 (3H, s, 6-CH<sub>3</sub>). <sup>13</sup>C NMR (125 MHz, DMSO-*d*<sub>6</sub>, ppm): δ 160.28, 147.57, 146.39, 137.43, 136.37, 136.19, 129.24, 129.23, 129.22, 129.21, 129.20, 129.19, 128.63, 128.50, 128.49, 127.60, 125.86, 124.25, 121.84, 53.31, 41.45, 21.28. ESI-MS *m/z*: 332.10 [M+H]<sup>+</sup>.

#### **3-((1-Benzyl-1H-1,2,3-triazol-4-yl)methyl)-7-methylquinazolin-4(3H)-one (4c)**

## Chem. Biodiversity

White solid; Yield: 67%. mp: 176–177 °C.  $R_f = 0.68$  (DCM : MeOH = 14 : 1). IR (KBr,  $cm^{-1}$ ): 3136, 3063 (CH, arene); 2955 (CH,  $CH_2$ ); 1661 (C=O); 1603, 1454 (C=C).  $^1H$ -NMR (500 MHz, DMSO- $d_6$ , ppm):  $\delta$  8.44 (1H, d,  $J = 8.00$  Hz, H-2); 8.11 (1H, d,  $J = 9.50$  Hz, H-6'); 7.93 (1H, d,  $J = 8.50$  Hz, H-5); 7.43 (1H, d,  $J = 5.50$  Hz, H-8); 7.29–7.21 (6H, m, H-6, H-3'', H-4'', H-5'', H-6'', H-7''); 5.47 (2H, d,  $J = 2.50$  Hz, H-1''a, H-1''b); 5.17 (2H, d,  $J = 6.50$  Hz, H-1'a, H-1'b); 2.37 (3H, s, 7- $CH_3$ ).  $^{13}C$  NMR (125 MHz, DMSO- $d_6$ , ppm):  $\delta$  160.21, 148.59, 145.50, 136.29, 129.21, 129.07, 128.64, 128.51, 127.34, 126.40, 124.47, 119.68, 53.38, 41.43, 21.76. ESI-MS  $m/z$ : 332.00 [M+H] $^+$ .

**3-((1-Benzyl-1H-1,2,3-triazol-4-yl)methyl)-7-methoxyquinazolin-4(3H)-one (4d)**

White solid; Yield: 58%. mp: 191–192 °C.  $R_f = 0.62$  (DCM : MeOH = 14 : 1). IR (KBr,  $cm^{-1}$ ): 3084 (CH, arene); 2972 (CH,  $CH_2$ ); 1674 (C=O); 1609, 1450 (C=C).  $^1H$ -NMR (500 MHz, DMSO- $d_6$ , ppm):  $\delta$  8.50 (1H, s, H-2); 8.15 (1H, s, H-6'); 7.95 (1H, d,  $J = 9.00$  Hz, H-5); 7.29–7.22 (6H, m, H-8, H-3'', H-4'', H-5'', H-6'', H-7''); 7.05 (1H, d,  $J = 9.00$  Hz, H-6); 5.48 (2H, d,  $J = 3.00$  Hz, H-1''a, H-1''b); 5.17 (2H, s, H-1'a, H-1'b); 3.81 (3H, s, 7-O $CH_3$ ).  $^{13}C$  NMR (125 MHz, DMSO- $d_6$ , ppm):  $\delta$  164.51, 129.23, 129.19, 128.92, 128.69, 128.55, 128.22, 117.45, 109.06, 56.35, 54.07, 53.47. ESI-MS  $m/z$ : 348.00 [M+H] $^+$ .

**3-((1-Benzyl-1H-1,2,3-triazol-4-yl)methyl)-6,7-dimethoxyquinazolin-4(3H)-one (4e)**

White solid; Yield: 54%. mp: 211–212 °C.  $R_f = 0.59$  (DCM : MeOH = 14 : 1). IR (KBr,  $cm^{-1}$ ): 3061 (CH, arene); 2970 (CH,  $CH_2$ ); 1662 (C=O); 1607, 1499 (C=C).  $^1H$ -NMR (500 MHz, DMSO- $d_6$ , ppm):  $\delta$  8.41 (1H, s, H-2); 8.13 (1H, d,  $J = 5.00$  Hz, H-6'); 7.31–7.22 (6H, m, H-5, H-3'', H-4'', H-5'', H-6'', H-7''); 7.13 (1H, s, H-8); 5.49 (2H, s, H-1''a, H-1''b); 5.18 (2H, s, H-1'a, H-1'b); 3.78 (3H, s, 7-O $CH_3$ ); 3.76 (3H, s, 6-O $CH_3$ ).  $^{13}C$  NMR (125 MHz, DMSO- $d_6$ , ppm):  $\delta$  159.53, 154.97, 149.33, 147.33, 144.20, 136.24, 129.23, 128.68, 128.56, 124.61, 115.06, 108.50, 105.51, 56.49, 56.18, 53.45, 41.58, 31.16. ESI-MS  $m/z$ : 378.10 [M+H] $^+$ .

**3-((1-Benzyl-1H-1,2,3-triazol-4-yl)methyl)-6-fluoroquinazolin-4(3H)-one (4f)**

White solid; Yield: 63%. mp: 181–182 °C.  $R_f = 0.65$  (DCM : MeOH = 14 : 1). IR (KBr,  $cm^{-1}$ ): 3061, 3028 (CH, arene); 2922 (CH,  $CH_2$ ); 1689 (C=O); 1605, 1483 (C=C).  $^1H$ -NMR (500 MHz, DMSO- $d_6$ , ppm):  $\delta$  8.47 (1H, s, H-2); 8.12 (1H, s, H-6'); 7.74–7.64 (3H, m, H-5, H-7, H-8); 7.29–7.21 (5H, m, H-3'', H-4'', H-5'', H-6'', H-7''); 5.48 (2H, s, H-1''a, H-1''b); 5.19 (2H, s, H-1'a, H-1'b).  $^{13}C$  NMR (125 MHz, DMSO- $d_6$ , ppm):  $\delta$  161.74, 159.78, 159.72, 147.91, 145.28, 136.33, 130.71, 130.64, 129.22, 128.65, 128.51, 127.93, 124.42, 123.52, 123.33, 111.30, 111.11, 53.35, 41.65. ESI-MS  $m/z$ : 336.00 [M+H] $^+$ .

**3-((1-Benzyl-1H-1,2,3-triazol-4-yl)methyl)-7-fluoroquinazolin-4(3H)-one (4g)**

White solid; Yield: 60%. mp: 185–186 °C.  $R_f = 0.65$  (DCM : MeOH = 14 : 1). IR (KBr,  $cm^{-1}$ ): 3107, 3061 (CH, arene); 2954 (CH,  $CH_2$ ); 1661 (C=O); 1603, 1477 (C=C).  $^1H$ -NMR (500 MHz, DMSO- $d_6$ , ppm):  $\delta$  8.53 (1H, s, H-2); 8.13 (1H, s, H-6'); 8.11–8.10 (1H, m, H-5); 7.43 (1H, d,  $J = 10.00$  Hz, H-6); 7.35–7.21 (6H, m, H-8, H-3'', H-4'', H-5'', H-6'', H-7''); 5.48 (2H, s, H-1''a, H-1''b); 5.18 (2H, s, H-1'a, H-1'b).  $^{13}C$  NMR (125 MHz, DMSO- $d_6$ , ppm):  $\delta$  167.08, 165.08, 163.37, 159.69, 150.46, 149.88, 136.29, 129.80, 129.71, 129.22, 128.65, 128.51, 127.93, 124.49, 119.13, 116.38, 116.19, 112.97, 112.80, 53.37, 41.60. ESI-MS  $m/z$ : 336.00 [M+H] $^+$ .

**3-((1-Benzyl-1H-1,2,3-triazol-4-yl)methyl)-6-chloroquinazolin-4(3H)-one (4h)**

White solid; Yield: 67%. mp: 191–192 °C.  $R_f = 0.64$  (DCM : MeOH = 14 : 1). IR (KBr,  $cm^{-1}$ ): 3107 (CH, arene); 2999, 2953 (CH,  $CH_2$ ); 1665 (C=O); 1605, 1472 (C=C).  $^1H$ -NMR (500 MHz, DMSO- $d_6$ , ppm):  $\delta$  8.50 (1H, s, H-2); 8.11 (1H, s, H-6'); 7.99 (1H, d,  $J = 2.50$  Hz, H-5); 7.78 (1H, dd,  $J = 9.00$  Hz,  $J' = 2.50$  Hz, H-7); 7.64 (1H, d,  $J = 9.00$  Hz, H-8); 7.28–7.21 (5H, m, H-3'', H-4'', H-5'', H-6'', H-7''); 5.47 (2H, s, H-1''a, H-1''b); 5.18 (2H, s, H-1'a, H-1'b).  $^{13}C$  NMR (125 MHz, DMSO- $d_6$ , ppm):  $\delta$  159.42, 148.89, 147.13, 142.98, 136.34, 135.07, 131.95, 130.05, 129.22, 128.64, 128.50, 125.52, 124.35, 123.32, 53.33, 41.72. ESI-MS  $m/z$ : 352.10 ( $^{35}Cl$ ), 354.00 ( $^{37}Cl$ ) [M+H] $^+$ .

**3-((1-Benzyl-1H-1,2,3-triazol-4-yl)methyl)-6-bromoquinazolin-4(3H)-one (4i)**

White solid; Yield: 63%. mp: 223–124 °C.  $R_f = 0.66$  (DCM : MeOH = 14 : 1). IR (KBr,  $cm^{-1}$ ): 3127, 3063 (CH, arene); 2945 (CH,  $CH_2$ ); 1676 (C=O); 1615, 1460 (C=C).  $^1H$ -NMR (500 MHz, DMSO- $d_6$ , ppm):  $\delta$  8.51 (1H, s, H-2); 8.12 (1H, d,  $J = 2.00$  Hz, H-5); 8.11 (1H, s, H-6'); 7.89 (1H, dd,  $J = 8.50$  Hz,  $J' = 2.50$  Hz, H-7); 7.56 (1H, d,  $J = 8.50$  Hz, H-8); 7.29–7.21 (5H, m, H-3'', H-4'', H-5'', H-6'', H-7''); 5.48 (2H, s, H-1''a, H-1''b); 5.18 (2H, s, H-1'a, H-1'b).  $^{13}C$  NMR (125 MHz, DMSO- $d_6$ , ppm):  $\delta$  159.29, 148.97, 147.40, 142.89, 137.77, 136.36, 130.16, 129.22, 128.64, 128.49, 124.29, 123.66, 120.12, 53.33, 41.73. ESI-MS  $m/z$ : 396.00 ( $^{79}Br$ ), 398.00 ( $^{81}Br$ ) [M+H] $^+$ .

**3-((1-Benzyl-1H-1,2,3-triazol-4-yl)methyl)-6-iodoquinazolin-4(3H)-one (4j)**

White solid; Yield: 65%. mp: 231–232 °C.  $R_f = 0.63$  (DCM : MeOH = 14 : 1). IR (KBr,  $cm^{-1}$ ): 3132, 3059 (CH, arene); 2986, 2930 (CH,  $CH_2$ ); 1665 (C=O); 1605, 1458 (C=C).  $^1H$ -NMR (500 MHz, DMSO- $d_6$ , ppm):  $\delta$  8.50 (1H, s, H-2); 8.32 (1H, d,  $J = 2.00$  Hz, H-5); 8.11 (1H, s, H-6'); 8.04 (1H, dd,  $J = 8.50$  Hz,  $J' = 2.00$  Hz, H-7); 7.41 (1H, d,  $J = 8.50$  Hz, H-8); 7.29–7.21 (5H, m, H-3'', H-4'', H-5'', H-6'', H-7''); 5.47 (2H, s, H-1''a, H-1''b); 5.17 (2H, s, H-1'a, H-1'b).  $^{13}C$  NMR (125 MHz, DMSO- $d_6$ , ppm):  $\delta$  159.10, 149.04, 147.68, 143.30, 136.35, 134.81, 129.93, 129.23, 128.65, 128.50, 124.34, 123.85, 92.81, 53.33, 41.74. ESI-MS  $m/z$ : 444.00 [M+H] $^+$ .

**General procedures for the synthesis of compounds 6a-j**

Compounds 6a-j were synthesized via a three-step pathway as illustrated in scheme 2. The first step was similar to that described for compounds 4a-j, followed by chlorination with thionyl chloride resulting in 4-chloro-quinazoline derivatives 5a-j. A mixture of compounds 2 and thionyl chloride was stirred at 120 °C for 5 hours. Then, the resulting mixtures were evaporated under reduced pressure to give the

## Chem. Biodiversity

residues, which were re-dissolved in 50 ml of water. After that, the mixtures were neutralised with a solution of NaHCO<sub>3</sub> 5% and extracted with DCM (3 × 15 mL). The organic layers were combined and filtered with anhydrous Na<sub>2</sub>SO<sub>4</sub>. The solvent was removed under reduced pressure to give the intermediates **5a-j**.

The 4-chloro-quinazolines were reacted with 1-benzylpiperidin-4-amine in the presence of K<sub>2</sub>CO<sub>3</sub>. A respective solution of the intermediates **5a-j** and 1-benzylpiperidin-4-amine (1 mmol) in 2-propanol (10 mL) were stirred at room temperature for 10 minutes, then K<sub>2</sub>CO<sub>3</sub> (165.5 mg, 1.2 mmol) was added. The mixture was stirred at 70°C until the reaction completed (5 hours). The resulting mixtures were evaporated under reduced pressure to give the residues, which were re-dissolved in 50 ml of DCM. The mixtures were filtered and the DCM layers were evaporated under reduced pressure to give the white solids. The crude products were further purified by column chromatography (DCM/methanol = 100 : 5) to give the target compounds **6a-j**.

**N-(1-Benzylpiperidin-4-yl)quinazolin-4-amine (6a)**

White solid; Yield: 69%. mp: 171-172 °C. *R<sub>f</sub>* = 0.46 (DCM : MeOH = 14 : 1). IR (KBr, cm<sup>-1</sup>): 3063 (CH, arene); 2951 (CH, CH<sub>2</sub>); 1580 (C=C). <sup>1</sup>H-NMR (500 MHz, DMSO-d<sub>6</sub>, ppm): δ 8.45 (1H, s, H-2); 8.31 (1H, d, *J* = 8.00 Hz, NH); 7.91 (1H, d, *J* = 7.50 Hz, H-5); 7.75 (1H, t, *J* = 8.00 Hz, H-7); 7.66 (1H, d, *J* = 8.00 Hz, H-8); 7.50 (1H, t, *J* = 7.25 Hz, H-6); 7.33-7.25 (5H, m, H-3", H-4", H-5", H-6", H-7"); 4.23-4.17 (1H, m, H-1'); 3.50 (2H, s, H-1"a, H-1"b); 2.89-2.87 (2H, m, H-3'a, H-5'a); 2.10-2.06 (2H, m, H-3'b, H-5'b); 1.93-1.90 (2H, m, H-2'a, H-6'a); 1.70-1.67 (2H, m, H-2'b, H-6'b). <sup>13</sup>C NMR (125 MHz, DMSO-d<sub>6</sub>, ppm): δ 159.20, 155.57, 149.68, 139.17, 132.91, 129.17, 128.64, 127.91, 127.32, 125.83, 123.34, 115.37, 62.61, 52.84, 48.39, 31.64. ESI-MS *m/z*: 319.20 [M+H]<sup>+</sup>.

**N-(1-Benzylpiperidin-4-yl)-6-methylquinazolin-4-amine (6b)**

White solid; Yield: 65%. mp: 185-186 °C. *R<sub>f</sub>* = 0.48 (DCM : MeOH = 14 : 1). IR (KBr, cm<sup>-1</sup>): 3026 (CH, arene); 2934 (CH, CH<sub>2</sub>); 1580 (C=C). <sup>1</sup>H-NMR (500 MHz, DMSO-d<sub>6</sub>, ppm): δ 8.40 (1H, s, H-2); 8.12 (1H, s, H-5); 7.89 (1H, d, *J* = 7.50 Hz, H-7); 7.60-7.57 (1H, m, H-8); 7.36-7.25 (5H, m, H-3", H-4", H-5", H-6", H-7"); 4.21-4.15 (1H, m, H-1'); 3.50 (2H, s, H-1"a, H-1"b); 2.88-2.86 (2H, m, H-3'a, H-5'a); 2.47 (3H, s, 6-CH<sub>3</sub>); 2.09-2.05 (2H, m, H-3'b, H-5'b); 1.92-1.90 (2H, m, H-2'a, H-6'a); 1.71-1.63 (2H, m, H-2'b, H-6'b). <sup>13</sup>C NMR (125 MHz, DMSO-d<sub>6</sub>, ppm): δ 158.82, 154.81, 147.93, 139.18, 135.37, 134.54, 129.17, 128.64, 127.73, 127.32, 122.27, 115.19, 62.60, 52.85, 48.34, 31.70, 21.59. ESI-MS *m/z*: 333.20 [M+H]<sup>+</sup>.

**N-(1-Benzylpiperidin-4-yl)-7-methylquinazolin-4-amine (6c)**

White solid; Yield: 67%. mp: 188-189 °C. *R<sub>f</sub>* = 0.49 (DCM : MeOH = 14 : 1). IR (KBr, cm<sup>-1</sup>): 3026 (CH, arene); 2938 (CH, CH<sub>2</sub>); 1574 (C=C). <sup>1</sup>H-NMR (500 MHz, DMSO-d<sub>6</sub>, ppm): δ 8.40 (1H, s, H-2); 8.20 (1H, d, *J* = 8.50 Hz, H-5); 7.82 (1H, d, *J* = 7.50 Hz, H-6); 7.46 (1H, s, H-8); 7.36-7.25 (5H, m, H-3", H-4", H-5", H-6", H-7"); 4.20-4.14 (1H, m, H-1'); 3.50 (2H, s, H-1"a, H-1"b); 2.88-2.86 (2H, m, H-3'a, H-5'a); 2.09 (3H, s, 7-CH<sub>3</sub>); 2.20-2.05 (2H, m, H-3'b, H-5'b); 1.92-1.89 (2H, m, H-2'a, H-6'a); 1.71-1.63 (2H, m, H-2'b, H-6'b). <sup>13</sup>C NMR (125 MHz, DMSO-d<sub>6</sub>, ppm): δ 159.07, 155.65, 149.89, 145.89, 143.01, 139.15, 129.19, 128.64, 127.56, 127.33, 127.11, 126.17, 123.15, 113.22, 62.60, 52.84, 48.31, 31.68, 21.74. ESI-MS *m/z*: 333.20 [M+H]<sup>+</sup>.

**N-(1-Benzylpiperidin-4-yl)-7-methoxyquinazolin-4-amine (6d)**

White solid; Yield: 54%. mp: 201-202 °C. *R<sub>f</sub>* = 0.45 (DCM : MeOH = 14 : 1). IR (KBr, cm<sup>-1</sup>): 3071 (CH, arene); 2947 (CH, CH<sub>2</sub>); 1582, 1566 (C=C). <sup>1</sup>H-NMR (500 MHz, DMSO-d<sub>6</sub>, ppm): δ 8.47 (1H, s, H-2); 8.33 (1H, d, *J* = 9.50 Hz, H-5); 8.01 (1H, d, *J* = 7.50 Hz, H-8); 7.45 (1H, t, *J* = 9.50 Hz, H-6); 7.36-7.25 (5H, m, H-3", H-4", H-5", H-6", H-7"); 4.21-4.18 (1H, m, H-1'); 4.02 (3H, s, 7-OCH<sub>3</sub>); 3.50 (2H, s, H-1"a, H-1"b); 2.89-2.86 (2H, m, H-3'a, H-5'a); 2.09-2.05 (2H, m, H-3'b, H-5'b); 1.92-1.89 (2H, m, H-2'a, H-6'a); 1.70-1.64 (2H, m, H-2'b, H-6'b). <sup>13</sup>C NMR (125 MHz, DMSO-d<sub>6</sub>, ppm): δ 162.77, 159.13, 158.90, 158.02, 156.72, 156.09, 152.00, 147.48, 139.16, 129.17, 128.64, 127.33, 124.94, 123.42, 116.89, 116.24, 112.18, 110.58, 109.54, 107.29, 62.57, 57.19, 55.93, 52.84, 52.81, 48.61, 48.26, 31.65. ESI-MS *m/z*: 349.10 [M+H]<sup>+</sup>.

**N-(1-Benzylpiperidin-4-yl)-6,7-dimethoxyquinazolin-4-amine (6e)**

White solid; Yield: 51%. mp: 231-232 °C. *R<sub>f</sub>* = 0.43 (DCM : MeOH = 14 : 1). IR (KBr, cm<sup>-1</sup>): 3132 (CH, arene); 2934 (CH, CH<sub>2</sub>); 1582 (C=C). <sup>1</sup>H-NMR (500 MHz, DMSO-d<sub>6</sub>, ppm): δ 8.32 (1H, s, H-2); 7.61 (1H, s, H-5); 7.57 (1H, d, *J* = 7.50 Hz, NH); 7.36-7.25 (5H, m, H-3", H-4", H-5", H-6", H-7"); 7.07 (1H, s, H-8); 4.20-4.17 (1H, m, H-1'); 3.99 (2H, s, H-1"a, H-1"b); 3.90 (3H, s, 7-OCH<sub>3</sub>); 3.89 (3H, s, 6-OCH<sub>3</sub>); 2.90-2.88 (2H, m, H-3'a, H-5'a); 2.10-2.06 (2H, m, H-3'b, H-5'b); 1.94-1.92 (2H, m, H-2'a, H-6'a); 1.71-1.64 (2H, m, H-2'b, H-6'b). <sup>13</sup>C NMR (125 MHz, DMSO-d<sub>6</sub>, ppm): δ 158.06, 154.16, 153.99, 148.74, 146.61, 139.24, 129.12, 128.65, 127.32, 108.89, 107.51, 102.54, 62.56, 56.61, 56.11, 52.95, 48.22, 32.03. ESI-MS *m/z*: 379.20 [M+H]<sup>+</sup>.

**N-(1-Benzylpiperidin-4-yl)-6-fluoroquinazolin-4-amine (6f)**

White solid; Yield: 61%. mp: 197-198 °C. *R<sub>f</sub>* = 0.54 (DCM : MeOH = 14 : 1). IR (KBr, cm<sup>-1</sup>): 3136, 3069 (CH, arene); 2941 (CH, CH<sub>2</sub>); 1584 (C=C). <sup>1</sup>H-NMR (500 MHz, DMSO-d<sub>6</sub>, ppm): δ 8.45 (1H, s, H-2); 8.20 (1H, dd, *J* = 10.25 Hz, *J'* = 2.75 Hz, H-5); 7.87 (1H, d, *J* = 7.00 Hz, NH); 7.76-7.73 (1H, m, H-7); 7.68-7.64 (1H, m, H-8); 7.35-7.25 (5H, m, H-3", H-4", H-5", H-6", H-7"); 4.18-4.15 (1H, m, H-1'); 3.49 (2H, s, H-1"a, H-1"b); 2.88-2.86 (2H, m, H-3'a, H-5'a); 2.09-2.04 (2H, m, H-3'b, H-5'b); 1.93-1.91 (2H, m, H-2'a, H-6'a); 1.69-1.62 (2H, m, H-2'b, H-6'b). <sup>13</sup>C NMR (125 MHz, DMSO-d<sub>6</sub>, ppm): δ 160.49, 158.97, 158.94, 158.56, 155.09, 155.08, 146.79, 139.13, 130.76, 130.69, 129.17, 128.63, 127.32, 122.33, 122.13, 115.82, 115.75, 107.84, 107.66, 62.59, 52.75, 48.54, 31.60, 31.14. ESI-MS *m/z*: 337.20 [M+H]<sup>+</sup>.

**N-(1-Benzylpiperidin-4-yl)-7-fluoroquinazolin-4-amine (6g)**

## Chem. Biodiversity

White solid; Yield: 63%. mp: 187-188 °C.  $R_f = 0.53$  (DCM : MeOH = 14 : 1). IR (KBr,  $\text{cm}^{-1}$ ): 3022 (CH, arene); 2926 (CH,  $\text{CH}_2$ ); 1591 (C=C).  $^1\text{H-NMR}$  (500 MHz,  $\text{DMSO-d}_6$ , ppm):  $\delta$  8.45 (1H, s, H-2); 8.43-8.40 (1H, m, H-5); 8.01 (1H, d,  $J = 7.50$  Hz, H-6); 7.42-7.23 (6H, m, H-8, H-3", H-4", H-5", H-6", H-7"); 4.20-4.16 (1H, m, H-1'); 3.48 (2H, s, H-1"a, H-1"b); 2.87-2.84 (2H, m, H-3'a, H-5'a); 2.09-2.03 (2H, m, H-3'b, H-5'b); 1.91-1.89 (2H, m, H-2'a, H-6'a); 1.70-1.63 (2H, m, H-2'b, H-6'b).  $^{13}\text{C NMR}$  (125 MHz,  $\text{DMSO-d}_6$ , ppm):  $\delta$  165.75, 163.76, 159.00, 156.71, 151.80, 151.70, 139.13, 129.15, 128.62, 127.30, 126.67, 126.59, 115.17, 114.98, 112.48, 111.86, 111.70, 62.58, 52.77, 48.48, 40.50, 40.26, 40.09, 31.61. ESI-MS  $m/z$ : 337.20  $[\text{M}+\text{H}]^+$ .

**N-(1-Benzylpiperidin-4-yl)-6-chloroquinazolin-4-amine (6h)**

White solid; Yield: 64%. mp: 194-195 °C.  $R_f = 0.54$  (DCM : MeOH = 14 : 1). IR (KBr,  $\text{cm}^{-1}$ ): 3086 (CH, arene); 2941 (CH,  $\text{CH}_2$ ); 1580 (C=C).  $^1\text{H-NMR}$  (500 MHz,  $\text{DMSO-d}_6$ , ppm):  $\delta$  8.50 (1H, d,  $J = 2.00$  Hz, H-2); 8.47 (1H, s, H-5); 8.03 (1H, d,  $J = 7.50$  Hz, NH); 7.76 (1H, dd,  $J = 8.75$  Hz,  $J' = 2.75$  Hz, H-7); 7.68 (1H, d,  $J = 8.50$  Hz, H-8); 7.35-7.25 (5H, m, H-3", H-4", H-5", H-6", H-7"); 4.19-4.13 (1H, m, H-1'); 3.49 (2H, s, H-1"a, H-1"b); 2.88-2.85 (2H, m, H-3'a, H-5'a); 2.09-2.04 (2H, m, H-3'b, H-5'b); 1.92-1.90 (2H, m, H-2'a, H-6'a); 1.67-1.64 (2H, m, H-2'b, H-6'b).  $^{13}\text{C NMR}$  (125 MHz,  $\text{DMSO-d}_6$ , ppm):  $\delta$  158.46, 155.95, 148.40, 139.11, 133.30, 130.12, 130.04, 129.17, 128.63, 127.32, 122.68, 116.19, 62.57, 52.74, 48.62, 31.54, 31.14. ESI-MS  $m/z$ : 353.10 ( $^{35}\text{Cl}$ ), 355.10 ( $^{37}\text{Cl}$ )  $[\text{M}+\text{H}]^+$ .

**N-(1-Benzylpiperidin-4-yl)-6-bromoquinazolin-4-amine (6i)**

White solid; Yield: 66%. mp: 211-212 °C.  $R_f = 0.55$  (DCM : MeOH = 14 : 1). IR (KBr,  $\text{cm}^{-1}$ ): 3061 (CH, arene); 2940 (CH,  $\text{CH}_2$ ); 1574 (C=C).  $^1\text{H-NMR}$  (500 MHz,  $\text{DMSO-d}_6$ , ppm):  $\delta$  8.64 (1H, d,  $J = 2.00$  Hz, H-2); 8.48 (1H, s, H-5); 8.06 (1H, d,  $J = 7.50$  Hz, NH); 7.87 (1H, dd,  $J = 9.00$  Hz,  $J' = 2.00$  Hz, H-7); 7.61 (1H, d,  $J = 9.00$  Hz, H-8); 7.35-7.25 (5H, m, H-3", H-4", H-5", H-6", H-7"); 4.17-4.14 (1H, m, H-1'); 3.48 (2H, d,  $J = 2.00$  Hz, H-1"a, H-1"b); 2.87-2.85 (2H, m, H-3'a, H-5'a); 2.09-2.04 (2H, m, H-3'b, H-5'b); 1.92-1.90 (2H, m, H-2'a, H-6'a); 1.69-1.64 (2H, m, H-2'b, H-6'b).  $^{13}\text{C NMR}$  (125 MHz,  $\text{DMSO-d}_6$ , ppm):  $\delta$  158.30, 156.00, 148.62, 139.13, 135.92, 130.24, 129.16, 128.63, 127.31, 125.81, 118.28, 116.71, 62.57, 52.75, 48.63, 31.55. ESI-MS  $m/z$ : 397.10 ( $^{79}\text{Br}$ ), 399.10 ( $^{81}\text{Br}$ )  $[\text{M}+\text{H}]^+$ .

**N-(1-Benzylpiperidin-4-yl)-6-iodoquinazolin-4-amine (6j)**

White solid; Yield: 62%. mp: 234-235 °C.  $R_f = 0.57$  (DCM : MeOH = 14 : 1). IR (KBr,  $\text{cm}^{-1}$ ): 3059 (CH, arene); 2945 (CH,  $\text{CH}_2$ ); 1572 (C=C).  $^1\text{H-NMR}$  (500 MHz,  $\text{DMSO-d}_6$ , ppm):  $\delta$  8.77 (1H, d,  $J = 2.00$  Hz, H-2); 8.47 (1H, s, H-5); 8.06 (1H, d,  $J = 7.50$  Hz, NH); 8.01 (1H, dd,  $J = 8.75$  Hz,  $J' = 1.75$  Hz, H-7); 7.45 (1H, d,  $J = 9.00$  Hz, H-8); 7.36-7.24 (5H, m, H-3", H-4", H-5", H-6", H-7"); 4.18-4.15 (1H, m, H-1'); 3.50 (2H, s, H-1"a, H-1"b); 2.88-2.86 (2H, m, H-3'a, H-5'a); 2.09-2.04 (2H, m, H-3'b, H-5'b); 1.92-1.90 (2H, m, H-2'a, H-6'a); 1.70-1.62 (2H, m, H-2'b, H-6'b).  $^{13}\text{C NMR}$  (125 MHz,  $\text{DMSO-d}_6$ , ppm):  $\delta$  157.97, 155.96, 148.88, 141.28, 139.15, 131.84, 130.03, 129.15, 128.64, 127.32, 117.21, 90.79, 62.55, 52.77, 48.60, 31.57. ESI-MS  $m/z$ : 445.10  $[\text{M}+\text{H}]^+$ .

**Bioactivity***AChE inhibition assay*

AChE inhibitory activity was measured using the Ellman's method as previously reported<sup>[44]</sup> with slight modifications. Briefly, to 60  $\mu\text{L}$  of 50 mM  $\text{NaH}_2\text{PO}_4$  buffer (pH 7.7) were added 10  $\mu\text{L}$  of respective assayed sample (at stock solution of 0.2 mM). Then, 10  $\mu\text{L}$  of enzyme (0.005 unit enzyme per well) was added. The resulting contents were mixed and pre-read at 405 nm, then the contents were pre-incubated for 10 min at 37 °C. The reaction in each well was initiated by the addition of 10  $\mu\text{L}$  of 0.5 mM substrate (acetylthiocholine iodide or butyrylthiocholine bromide) to each well, followed by the addition of 10  $\mu\text{L}$  DTNB (0.5 mM per well). The wells were incubated for at 37 °C, then the absorbance of each well was measured at 412 nm using 96-well plate reader Synergy HT, Biotek, USA. All experiments were carried out in triplicate. Donepezil (0.2 mM stock solution) was used as a positive control. The inhibition percentages were calculated by the following formula:

$$\text{Inhibition percentage} = \frac{\text{Control}_{\text{Abs}} - \text{Sample}_{\text{Abs}}}{\text{Control}_{\text{Abs}}} \times 100$$

$\text{IC}_{50}$  values (in case measured) were calculated using EZ-Fit Enzyme kinetics software (Perrella Scientific Inc. Amherst, USA).

*DPPH radical scavenging assay*

1,1-Diphenyl-2-picrylhydrazyl (DPPH) radical-scavenging activity was measured according to a described method.<sup>[45]</sup> Briefly, 5  $\mu\text{L}$  of each sample dissolved in MeOH were added to 195  $\mu\text{L}$  of 150  $\mu\text{M}$  methanolic DPPH in 96-well plates. The solution was mixed for 1 min and incubated at room temperature in a dark place. After 30 min, the absorbance of the reaction mixture was measured at 520 nm on a microplate reader. The scavenging activity was expressed as the degree of radical reduction of a test group, in comparison to that of the control.

*Cytotoxicity assay*

## Chem. Biodiversity

The cytotoxicity of the synthesized compounds was evaluated against three human cancer cell lines, including SW620 (colon cancer), PC<sub>3</sub> (prostate cancer), and NCI-H23 (lung cancer). The cell lines were purchased from a Cancer Cell Bank at the Korea Research Institute of Bioscience and Biotechnology (KRIBB). The media, sera and other reagents that were used for cell culture in this assay were obtained from GIBCO Co. Ltd. (Grand Island, New York, USA). The cells were culture in DMEM (Dulbecco's Modified Eagle Medium) until confluence. The cells were then trypsinized and suspended at  $3 \times 10^4$  cells/mL of cell culture medium. On day 0, each well of the 96-well plates was seeded with 180  $\mu$ L of cell suspension. The plates were then incubated in a 5% CO<sub>2</sub> incubator at 37 °C for 24 h. Compounds were initially dissolved in dimethyl sulfoxide (DMSO) and diluted to appropriate concentrations by culture medium. Then 20  $\mu$ L of each compounds' samples, which were prepared as described above, were added to each well of the 96-well plates, which had been seeded with cell suspension and incubated for 24-h, at various concentrations. The plates were further incubated for 48 h. Cytotoxicity of the compounds was measured by the colorimetric method, as described previously<sup>[16]</sup> with slight modifications.<sup>[17-20]</sup> The IC<sub>50</sub> values were calculated using a Probits method<sup>[21]</sup> and were averages of three independent determinations (SD  $\leq$  10%).

### Cell cycle analysis

SW620 human colon cancer cells ( $2 \times 10^5$ /ml per well) were plated in 6-well culture plates and allowed to grow for 24 h. The cells were treated with compounds at appropriate concentrations for 24 h, respectively, and then harvested. The harvested cells were washed twice with ice-cold PBS, fixed in 75% ice-cold ethanol, and stained with propidium iodide (PI) in the presence of RNase at room temperature for 30 min. The stained cells were analyzed for DNA content using a FACScalibur flow cytometer (BD Biosciences, San Jose, CA, USA) and the data were processed using Cell Quest Pro software (BD Biosciences).

### Apoptosis assay

The Annexin V-FITC/PI dual staining assay was used to determine the percentage of apoptotic cells. SW620 human colon cancer cells ( $2 \times 10^5$ /ml per well) were plated in 6-well culture plates and allowed to grow for 24 h. The cells were treated with compounds at appropriate concentrations for 24 h, respectively, and then harvested. The harvested cells were washed twice with ice-cold PBS and incubated in the dark at room temperature in 100 ml of 1 $\times$  binding buffer containing 1  $\mu$ L Annexin V-FITC and 12.5 mL PI. After 15 min incubation, cells were analyzed for percentage undergoing apoptosis using a FACScalibur flow cytometer (BD Biosciences). The data were processed using Cell Quest Pro software (BD Biosciences).

### Molecular docking studies

The X-ray crystal structure of AChE-donepezil complex was retrieved from Protein Data bank (PDB ID: 4EY7) [10]. This protein structure is then prepared by retaining chain A and removing water molecules, correcting protein structure errors, protonating the structure, setting tethers of different strengths on the receptors, fixing atoms beyond a 8 distance-distance from the active site and finally optimizing the fixed structure by minimizing the structure to an RMS gradient of 0.1 kcal/mol/Å.<sup>[12, 22]</sup> The AMBER99 force field is added and the partial charge is recalculated for all atoms. All protein preparations were performed using MOE 2015.10 software.<sup>[12, 17, 23]</sup> The 2D structures of new compounds were built by using Marvin Sketch software and optimized by MOE energy minimizing mode. Molecular docking was performed using ICM-Pro 3.8-3 software (<http://www.molsoft.com/icmpro/>).<sup>[9, 24]</sup> Before performing docking studies, protocol docking was validated by re-docking the co-crystal ligands Donepezil. The suitability of the docking procedures was assessed via calculating RMSD between redocked and co-crystal ligand. The docking poses were selected based on the ICM scores and interaction profiles.

## Supplementary Material

Supporting information for this article is available on the WWW under <http://dx.doi.org/10.1002/MS-number>.

## Acknowledgements

We acknowledge the principal financial supports from the National Foundation for Science and Technology of Vietnam (NAFOSTED, Grant number 104.01-2018.301). The work was also partly supported by a grant funded by the Korean Government (NRF, Grant number 2017R1A5A2015541).

## Author Contribution Statement

## Chem. Biodiversity

N. T. T., N-H. N and S-B. H. proposed the work. N-H. N, T. T. L., and D. T. A. mainly developed the synthesis studies, S-B. H, E. J. P., J. S. K., J. H. K, and S. D. J. performed the biological testing assays. P-T. H., and D. T. M. D. performed the docking simulations and physicochemical computations. All authors read and approved the final manuscript.

## References

- [1] A. Kumar, A. Singh, Ekavali, 'A review on Alzheimer's disease pathophysiology and its management: an update', *Pharmacological Reports* **2015**, *67*, 195-203.
- [2] Y. Huang, L. Mucke, 'Alzheimer Mechanisms and Therapeutic Strategies', *Cell* **2012**, *148*, 1204-1222.
- [3] K. G. Yiannopoulou, S. G. Papageorgiou, 'Current and future treatments for Alzheimer's disease', *Therapeutic Advances in Neurological Disorders* **2012**, *6*, 19-33.
- [4] G. Olivero, M. Grilli, J. Chen, S. Preda, E. Mura, S. Govoni, M. Marchi, 'Effects of soluble  $\beta$ -amyloid on the release of neurotransmitters from rat brain synaptosomes', *Frontiers in Aging Neuroscience* **2014**, *6*, 166.
- [5] J. Rodda, J. Carter, 'Cholinesterase inhibitors and memantine for symptomatic treatment of dementia', *BMJ : British Medical Journal* **2012**, *344*, e2986.
- [6] J. Massoulié, L. Pezzementi, S. Bon, E. Krejci, F.-M. Vallette, 'Molecular and cellular biology of cholinesterases', *Progress in Neurobiology* **1993**, *41*, 31-91.
- [7] M. Singh, M. Kaur, H. Kukreja, R. Chugh, O. Silakari, D. Singh, 'Acetylcholinesterase inhibitors as Alzheimer therapy: From nerve toxins to neuroprotection', *Eur J Med Chem* **2013**, *70*, 165-188.
- [8] M. Asif, 'Chemical Characteristics, Synthetic Methods, and Biological Potential of Quinazoline and Quinazolinone Derivatives', *International Journal of Medicinal Chemistry* **2014**, *2014*, 395637.
- [9] M. A. C. Neves, M. Totrov, R. Abagyan, 'Docking and scoring with ICM: the benchmarking results and strategies for improvement', *J Comput Aided Mol Des* **2012**, *26*, 675-686.
- [10] J. Cheung, M. J. Rudolph, F. Burshteyn, M. S. Cassidy, E. N. Gary, J. Love, M. C. Franklin, J. J. Height, 'Structures of Human Acetylcholinesterase in Complex with Pharmacologically Important Ligands', *J Med Chem* **2012**, *55*, 10282-10286.
- [11] B. C. Roberts, R. L. Mancera, 'Ligand-Protein Docking with Water Molecules', *J Chem Inf Model* **2008**, *48*, 397-408.
- [12] T. T. Lan, D. T. Anh, P.-T. Hai, D. T. M. Dung, L. T. T. Huong, E. J. Park, H. W. Jeon, J. S. Kang, N. T. Thuan, S.-B. Han, N.-H. Nam, 'Design, synthesis, and bioevaluation of novel oxoindolin-2-one derivatives incorporating 1-benzyl-1H-1,2,3-triazole', *Medicinal Chemistry Research* **2020**, *29*, 396-408.
- [13] Y. Bourne, P. Taylor, Z. Radić, P. Marchot, 'Structural insights into ligand interactions at the acetylcholinesterase peripheral anionic site', *The EMBO Journal* **2003**, *22*, 1-12.
- [14] G. L. Ellman, K. D. Courtney, V. Andres, R. M. Featherstone, 'A new and rapid colorimetric determination of acetylcholinesterase activity', *Biochem Pharmacol* **1961**, *7*, 88-95.
- [15] T. Phuong Thien, N. Min-Kyun, D. Nguyen Hai, H. Tran Manh, K. Pham Thanh, T. Tran Van, N. Nguyen Hai, T. Nguyen Duy, S. Dai-Eun, B. Ki-Hwan, 'Antioxidant Activities of Vietnamese Medicinal Plants', *Natural Product Sciences* **2006**, *12*, 29-37.
- [16] P. Skehan, R. Storeng, D. Scudiero, A. Monks, J. McMahon, D. Vistica, J. T. Warren, H. Bokesch, S. Kenney, M. R. Boyd, 'New Colorimetric Cytotoxicity Assay for Anticancer-Drug Screening', *JNCL: Journal of the National Cancer Institute* **1990**, *82*, 1107-1112.
- [17] N.H. Nam, D.H. Hong, Y.J. You, Y. Kim, S.C. Bang, H.M. Kim, B.Z. Ahn. 'Synthesis and cytotoxicity of 2, 5-dihydroxychalcones and related compounds', *Arch Pharm Res* **2004**, *27*, 581-589.
- [18] N.-H. Nam, T. L. Huong, D. T. M. Dung, P. T. P. Dung, D. T. K. Oanh, S. H. Park, K. Kim, B. W. Han, J. Yun, J. S. Kang, Y. Kim, S.-B. Han, 'Synthesis, bioevaluation and docking study of 5-substitutedphenyl-1,3,4-thiadiazole-based hydroxamic acids as histone deacetylase inhibitors and antitumor agents', *J Enzyme Inhib Med Chem* **2014**, *29*, 611-618.
- [19] B.-S. Min, H.-T.-T. Huong, J.-H. Kim, H.-J. Jun, M.-K. Na, N.-H. Nam, H.-K. Lee, K. H. Bae, S.-S. Kang, 'Furo-1,2-naphthoquinones from *Crataegus pinnatifida* with ICAM-1 Expression Inhibition Activity', *Planta Med* **2004**, *70*, 1166-1169.
- [20] N.-H. Nam, R. L. Pitts, G. Sun, S. Sardari, A. Tiemo, M. Xie, B. Yan, K. Parang, 'Design of tetrapeptide ligands as inhibitors of the Src SH2 domain', *Bioorg. Med. Chem.* **2004**, *12*, 779-787.

**Chem. Biodiversity**

- [21] L. Wu, A. M. Smythe, S. F. Stinson, L. A. Mullendore, A. Monks, D. A. Scudiero, K. D. Paull, A. D. Koutsoukos, L. V. Rubinstein, M. R. Boyd, R. H. Shoemaker, 'Multidrug-resistant Phenotype of Disease-oriented Panels of Human Tumor Cell Lines Used for Anticancer Drug Screening', *Cancer Res* **1992**, *52*, 3029-3034.
- [22] D. T. Hieu, D. T. Anh, P.-T. Hai, L.-T.-T. Huong, E. J. Park, J. E. Choi, J. S. Kang, P. T. P. Dung, S.-B. Han, N.-H. Nam, 'Quinazoline-Based Hydroxamic Acids: Design, Synthesis, and Evaluation of Histone Deacetylase Inhibitory Effects and Cytotoxicity', *Chem Biodivers* **2018**, *15*, e1800027.
- [23] Molecular Operating Environment (MOE), '2009.10; Chemical Computing Group ULC, 1010 Sherbooke St. West, Suite #910, Montreal, QC, Canada, H3A 2R7', **2009**.
- [24] J. An, M. Totrov, R. Abagyan, 'Pocketome via Comprehensive Identification and Classification of Ligand Binding Envelopes', *Molecular & Cellular Proteomics* **2005**, *4*, 752-761.